ELSEVIER

Biochemical Pharmacology 63 (2002) 199–206

Biochemical Pharmacology

Inhibitory effect of the plant-extract osthole on L-type calcium current in NG108-15 neuronal cells

Sheng-Nan Wu[a,b,*], Yuk-Kang Lo[c,d], Chien-Chich Chen[e], Hui-Fang Li[a], Hung-Ting Chiang[f]

[a]*Department of Medical Education and Research, Kaohsiung Veterans General Hospital, 386 Ta-Chung 1st Road, Kaohsiung City 813, Taiwan, ROC*
[b]*Institute of Biomedical Sciences, National Sun Yat-Sen University, Kaohsiung City, Taiwan, ROC*
[c]*Section of Neurology, Kaohsiung-Veterans General Hospital, Kaohsiung City, Taiwan, ROC*
[d]*National Yang-Ming University, Taipei, Taiwan, ROC*
[e]*National Institute of Chinese Medicine, Taipei, Taiwan, ROC*
[f]*Department of Internal Medicine, Kaohsiung-Veterans General Hospital, Kaohsiung City, Taiwan, ROC*

Received 16 March 2001; accepted 8 October 2001

Abstract

The effects of osthole, a coumarin isolated from *Cnidium monnieri* (L.) Cusson, on ionic currents in a mouse neuroblastoma and rat glioma hybrid cell line, NG105-18, were investigated with the aid of the whole-cell voltage-clamp technique. Osthole (0.3–100 μM) caused an inhibition of voltage-dependent L-type Ca^{2+} current ($I_{Ca,L}$) in a concentration-dependent manner. Osthole produced no change in the overall shape of the current–voltage relationship of $I_{Ca,L}$. The IC_{50} value of the osthole-induced inhibition of $I_{Ca,L}$ was 4 μM. The presence of osthole (3 μM) shifted the steady state inactivation curve of $I_{Ca,L}$ to a more negative potential by approximately −15 mV. Osthole (3 μM) also produced a prolongation in the recovery of $I_{Ca,L}$ inactivation. Although osthole might suppress phosophodiesterases to increase intracellular adenosine-3′,5′-cyclic monophosphate (cyclic AMP) or guanosine-3′,5′-cyclic monophosphate (cyclic GMP), sp-cAMPS did not affect $I_{Ca,L}$ and 8-bromo-cyclic GMP slightly suppressed it. Thus, osthole-mediated inhibition of $I_{Ca,L}$ was not associated with intracellular cyclic AMP or GMP. However, no effect of osthole on voltage-dependent K^+ outward current was observed. Under a current-clamp mode, osthole could decrease the firing frequency of action potentials. Therefore, the channel-blocking properties of osthole may, at least in part, contribute to the underlying mechanisms by which it affects neuronal or neuroendocrine function.

Keywords: Osthole; L-type Ca^{2+} current; Membrane potential; NG105-18 cells

1. Introduction

Osthole (7-methoxy-8-[3-methylpent-2-enyl]coumarin), a coumarin compound isolated from *Cnidium monnieri* (L.) Cusson, possesses a wide spectrum of pharmacological activities [1,2]. A previous report showed that osthole-inhibited ATP release induced by collagen, platelet-activating factor and arachidonic acid in rabbit platelets [3]. Osthole was also found to inhibit vascular smooth muscle contraction evoked by high K^+ as well as norepinephrine [4]. Previous findings thus suggested that osthole might be able to inhibit voltage-dependent Ca^{2+} channels in various tissues, including rat thoracic aorta, guinea pig trachea, guinea pig atrium and rabbit corpus cavernosum [1–8]. In addition, because osthole appeared to act like an inhibitor of cyclic nucleotide phosphodiesterases, the underlying mechanism of its actions was thought to be associated with a change in the level of intracellular cyclic AMP or GMP [5,7]. However, to our knowledge, the effects of osthole on ionic currents have not been studied.

NG108-15 neuroblastoma × glioma hybrid cells were used in the present study. This cell line is known to express at least three types of Ca^{2+} currents. These can be distinguished by their voltage-dependence of activation into a low-threshold T-type, and at least two types of Ca^{2+}

* Corresponding author.
Tel.: +886-7-342-2121/1507; fax: +886-7-346-8056.
E-mail address: snwu@isca.vghks.gov.tw (S.-N. Wu).

Abbreviations: Cyclic AMP, adenosine-3′,5′-cyclic monophosphate; Cyclic GMP, guanosine-3′,5′-cyclic monophosphate; 8-Bromo-cGMP, 8-bromoguanosine-3′,5′-cyclic monophosphate; $I_{Ca,L}$, voltage-dependent L-type Ca^{2+} current; I_K, voltage-dependent K^+ current; *I–V*, current–voltage; sp-cAMPS, sp-adenosine-3′,5′-cyclic monophosphorothioate; TEA, tetraethylammonium chloride; τ_{act}, activation time constant; $\tau_{inact(f)}$, fast component of inactivation time constant; $\tau_{inact(s)}$, slow component of inactivation time constant.

0006-2952/02/$ – see front matter
PII: S0006-2952(01)00873-5

channel contributing high-threshold Ca^{2+} current (I_{Ca}): an ω-conotoxin GVIA-resistant, dihydropyridine-sensitive type, an ω-conotoxin GVIA-sensitive, dihydropyridine-resistant type [9,10]. The amplitude of high-threshold I_{Ca} present in these cells was also regulated by Ca^{2+}-dependent phosphorylation, the activation of various G protein(s)-linked receptors, or the level of intracellular cADP-ribose [11–13]. Therefore, in the present study, we attempted to examine the ionic mechanisms by which osthole causes any effects on NG108-15 neuronal cells.

2. Materials and methods

2.1. Cell preparation

The clonal strain NG108-15 cell line, originally formed by Sendai virus-induced fusion of the mouse neuroblastoma clone N18TG-2 and the rat glioma clone C6 BV-1, was obtained from European Collection of Cell Cultures. Cells were grown in monolayer culture in 50 mL plastic culture flasks in a humidified environment of 5% CO_2/95% air at 37°. Cells were maintained at a density of 10^6/mL in 5 mL Dulbecco's modified Eagle's medium supplemented with 10% heat-inactivated fetal bovine serum (v/v), and 2 mM L-glutamine. Experiments were performed after 5 or 6 days of subcultivation (60–80% confluence).

2.2. Electrophysiological measurements

Immediately before each experiment, NG108-15 cells were dissociated and an aliquot of cell suspension was transferred to a recording chamber positioned on the stage of an inverted microscope (Diaphot-200; Nikon). The microscope was coupled to a video camera system with magnification up to 1500× to monitor cell size during the experiments. Cells were bathed at room temperature (20–25°) in normal Tyrode's solution containing 1.8 mM $CaCl_2$. Patch pipettes were pulled from borosilicate glass capillaries (Kimax-51) using a vertical two-stage electrode puller (PB-7, Narishige) and the tips were fire-polished with a microforge (MF-83; Narishige). The pipette used had a resistance of 3–5 MΩ when immersed in normal Tyrode's solution. Ion currents were measured with glass pipettes in the whole-cell configuration of the patch-clamp technique, using an RK-400 patch-clamp amplifier (Biologic) [14,15]. All potentials were corrected for liquid junction potential, a value that would develop at the tip of the pipette when the composition of the pipette solution was different from that in the bath.

2.3. Data recording and analysis

The signals consisting of voltage and current tracings were monitored with a digital storage oscilloscope (Model 1602; Gould) and simultaneously stored in a Pentium-III personal computer (TravelMate 525TE; Acer). The currents were filtered at 1 kHz. The data were digitized at 10 kHz with a Digidata 1320A device (Axon Instruments) controlled by the Clampex subroutine of the pCLAMP 8.02 software package (Axon Instruments). Voltage-activated currents recorded during whole-cell experiments were analyzed using the Clampfit subroutine (Axon Instruments) or the Origin 6.0 software package (Microcal Software Inc.) to establish a current–voltage (*I–V*) relationship for ionic currents.

To calculate the percentage inhibition of osthole, each cell was depolarized from a holding potential of −50 to +10 mV, the amplitude of $I_{Ca,L}$ after addition of osthole was compared with the control value. The concentration-dependent effect of osthole on the inhibition of $I_{Ca,L}$ was fitted with a Hill function using non-linear least-square regression [16]. That is, percentage inhibition $= (E_{max} \times [C]^n)/(IC_{50}^n + [C]^n)$, where $[C]$ represents the osthole concentration; IC_{50} and n are the concentration of osthole needed to reduce the current by 50% and the Hill coefficient, respectively; E_{max} is osthole-induced maximal inhibition of $I_{Ca,L}$.

The values for activation time constant (τ_{act}), fast component of inactivation time constant ($\tau_{inact(f)}$) and slow component of inactivation time constant ($\tau_{inact(s)}$) of $I_{Ca,L}$ were calculated by fitting currents to a single- or two-exponential function. Curve-fitting and parameter estimation were carried out using the Origin 6.0 software (Microcal). When cells were held at the level of −50 mV and the depolarizing pulses to +10 mV with a duration of 300 ms, the presence of osthole (3 μM) did not produce any significant change in the kinetics of activation or inactivation of $I_{Ca,L}$ (control: $\tau_{act} = 5.4 \pm 0.7$ ms, $\tau_{inact(f)} = 11.8 \pm 2.2$ ms, $\tau_{inact(s)} = 35.8 \pm 6.2$ ms; osthole: $\tau_{act} = 5.4 \pm 0.9$, $\tau_{inact(f)} = 11.4 \pm 2.3$ ms, $\tau_{inact(s)} = 35.2 \pm 5.5$ ms ($N = 8$)).

All values are reported as means ± SEM and error bars are plotted as SEM. The paired or unpaired Student's *t*-test and one way analysis of variance with a least-significance difference method for multiple comparisons were used for the statistical evaluation of differences among means. A value of $P < 0.05$ was considered to be statistically significant.

2.4. Drugs and solutions

Osthole was chemically purified as described previously and provided by Chien-Chich Chen [8]. Osthole was dissolved in dimethyl sulfoxide (less than 0.1%) and made immediately prior to experiments. Tetrodotoxin, TEA, and quinidine were purchased from Sigma Chemical Co. The sp-adenosine-3′,5′-cyclic monophosphorothioate (sp-cAMPS), 8-bromoguanosine-3′,5′-cyclic monophosphate (8-bromo-cGMP), and ω-conotoxin GVIA were obtained from Biomol. Nimodipine was purchased from Tocris Cookson Ltd. Dendrotoxin was obtained from Calbiochem. Tissue culture media, L-glutamine, penicillin–streptomycin, fungizone, and trypsin were obtained from

Life Technologies. All other chemicals were commercially available and of reagent grade. The composition of normal Tyrode's solution was as follows (in mM): NaCl 136.5, KCl 5.4, $CaCl_2$ 1.8, $MgCl_2$ 0.53, glucose 5.5 and HEPES–NaOH buffer 5.5 (pH 7.4). To record membrane potential or K^+ current, the patch pipettes were filled with a solution (in mM): K-aspartate 130, KCl 20, KH_2PO_4 1, $MgCl_2$ 1, EGTA 0.1, Na_2ATP 3, Na_2GTP 0.1 and HEPES–KOH buffer 5 (pH 7.2). To measure Ca^{2+} current, K^+ ions inside the pipette solution were replaced with equimolar Cs^+ ions, and pH was adjusted to 7.2 with CsOH.

3. Results

3.1. Effect of osthole on $I_{Ca,L}$ in NG105-18 cells

The effect of osthole on the amplitude of $I_{Ca,L}$ was examined in this study. In these experiments, cells were bathed in normal Tyrode's solution containing 1.8 mM $CaCl_2$ and the recording pipettes were filled with Cs^+-containing solution. As shown in Fig. 1, the effect of osthole on $I_{Ca,L}$ was studied at various membrane potentials, and an *I–V* relationship of $I_{Ca,L}$ was then constructed. By comparing the two *I–V* curves shown in Fig. 1, it can be seen that the threshold potential (around −30 mV), the potential of maximum peak $I_{Ca,L}$ (around +10 mV), and the apparent reversal potential (around +50 mV) were essentially the same in the absence and presence of osthole (10 μM). In other words, osthole (10 μM) was capable of suppressing the amplitude of $I_{Ca,L}$ without causing a shift in the *I–V* relationship for $I_{Ca,L}$. The inhibitory effect of osthole on $I_{Ca,L}$ was completely reversible. Similar results were also obtained from 10 different cells.

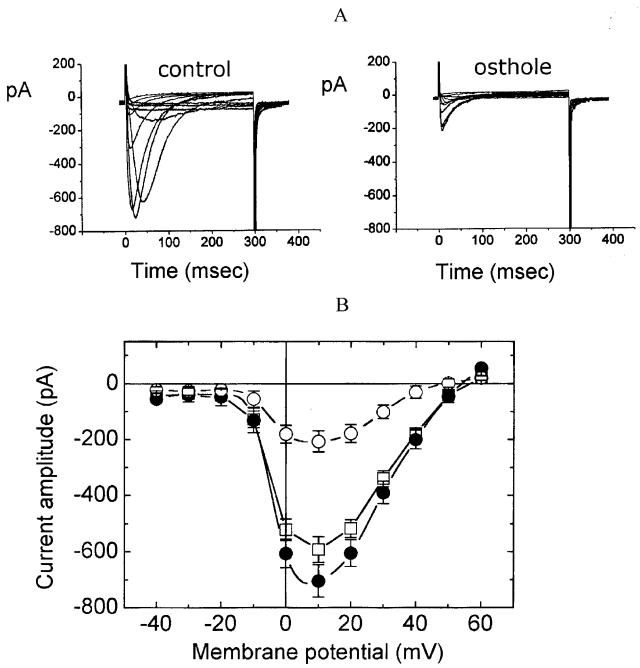

Fig. 1. The *I–V* relationships of $I_{Ca,L}$ in the absence and presence of osthole in NG108-15 cells. Patch pipette was loaded with Cs^+-containing solution and cells were bathed in normal Tyrode's solution containing 1.8 mM $CaCl_2$ and 10 mM TEA. (A) Superimposed current traces obtained in the absence (left) and presence (right) of osthole (10 μM). The cell was held at −50 mV and the voltage pulses from −40 to +60 mV in 10 mV increments were applied. (B) Averaged *I–V* relationship of the peak $I_{Ca,L}$ in control (filled circles), during exposure to 10 μM osthole (open circles) and during the washout of osthole (open squares). (mean ± SEM; N = 7–10 for each point).

Fig. 2 shows the relationship between the concentration of osthole and the percentage inhibition of $I_{Ca,L}$. Osthole (0.3–100 μM) suppressed the amplitude of $I_{Ca,L}$ in a concentration-dependent manner. The IC_{50} value for osthole-

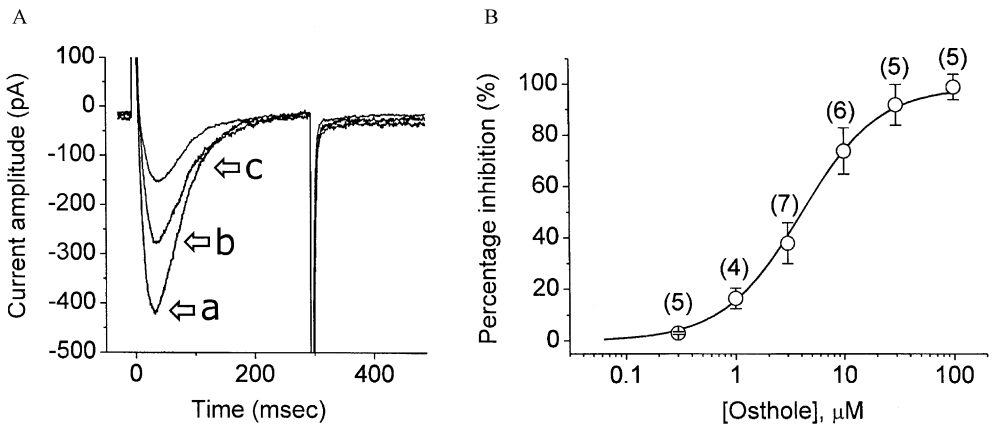

Fig. 2. Concentration-dependent inhibition of $I_{Ca,L}$ by osthole in NG108-15 cells. (A) Superimposed current traces obtained in the absence and presence of osthole. Cells were bathed in normal Tyrode's solution containing 1.8 mM $CaCl_2$ and the depolarizing pulses from −50 to +10 mV were applied with a duration of 300 ms. Labeled (a) is the control, labeled (b) and (c) were obtained after addition of 3 and 10 μM osthole, respectively. (B) Concentration–response relationship for osthole-induced inhibition of $I_{Ca,L}$. Each cell was held at the level of −50 mV, and the voltage pulses to +10 mV were applied. Various concentrations of osthole (0.3–100 μM) were examined. The amplitude of the peak $I_{Ca,L}$ during the application of osthole was compared with the control value. Parentheses shown in this and the following figures denote the number of cells examined. The smooth line represents the best fit to the Hill equation as described in Section 2. The values for IC_{50} and maximally inhibited percentage of $I_{Ca,L}$ in the presence of osthole were 4 μM and 99%, respectively. The Hill coefficient was 1.2.

induced inhibition of $I_{Ca,L}$ was 4 and 100 μM osthole fully suppressed the amplitude of $I_{Ca,L}$. The results clearly indicate that osthole has a depressant action on $I_{Ca,L}$ in NG108-15 neuronal cells.

3.2. Effects of sp-cAMPS, 8-bromo-cGMP, ω-conotoxin GVIA, nimodipine and osthole on the amplitude of $I_{Ca,L}$

It has previously been reported that osthole inhibits phosphodiesterase activity, resulting in an increase in the level of intracellular cyclic AMP or GMP [5,7]. Therefore, we examined whether cell permeable analogues of cyclic AMP and GMP affect the amplitude of $I_{Ca,L}$ present in NG108-15 cells. Fig. 3 shows the effect of sp-cAMPS and 8-bromo-cGMP on $I_{Ca,L}$. The sp-cAMPS (1 mM) had no effect on $I_{Ca,L}$ while 8-bromo-cGMP (1 mM) slightly suppressed it by about 15%. The sp-cAMPS and 8-bromo-cGMP are cell permeable analogues of cyclic AMP and GMP, respectively. In addition, ω-conotoxin GVIA (3 μM), a blocker of N-type Ca^{2+} channels [17], had no effect on $I_{Ca,L}$, whereas nimodipine (10 μM), a blocker of L-type Ca^{2+} channels, effectively suppressed the amplitude of $I_{Ca,L}$. Although sp-cAMPS or ω-conotoxin GVIA alone did not affect $I_{Ca,L}$, the application of osthole in the continued presence of sp-cAMPS or ω-conotoxin GVIA could suppress $I_{Ca,L}$ effectively. These findings indicate that Ca^{2+} current is sensitive to the inhibition by osthole, but not by sp-cAMPS or ω-conotoxin GVIA, and that osthole-induced inhibition of $I_{Ca,L}$ does not appear to involve intracellular cyclic AMP or GMP in these cells.

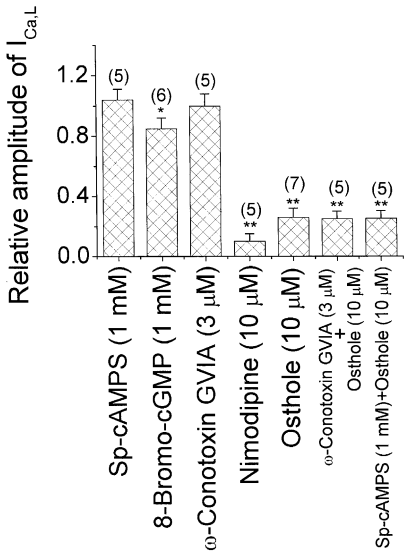

Fig. 3. Comparison between the effect of osthole and those of sp-cAMPS, 8-bromo-cGMP, ω-conotoxin GVIA, nimodipine, ω-conotoxin GVIA plus osthole, and sp-cAMPS plus osthole on the inhibition of $I_{Ca,L}$ in NG108-15 neuronal cells. Each cell was held at –50 mV and the depolarizing pulses to +10 mV (300 ms in duration) were applied at 0.05 Hz. The amplitude of $I_{Ca,L}$ in the control was considered to be 1.0 and the relative amplitude after application of each agent was plotted. In the experiments with ω-conotoxin GVIA plus osthole or sp-cAMPS plus osthole, osthole was applied after the addition of ω-conotoxin GVIA or sp-cAMPS. Mean ± SEM. *Significantly different ($P < 0.05$) from control. **Significantly different ($P < 0.01$) from control.

3.3. Voltage-dependence of osthole-induced inhibition of $I_{Ca,L}$

To characterize the inhibitory effects of osthole on $I_{Ca,L}$, we examined the voltage-dependence of the effect of osthole on $I_{Ca,L}$. Fig. 4 shows the steady state inactivation curve of $I_{Ca,L}$ in the absence and presence of osthole

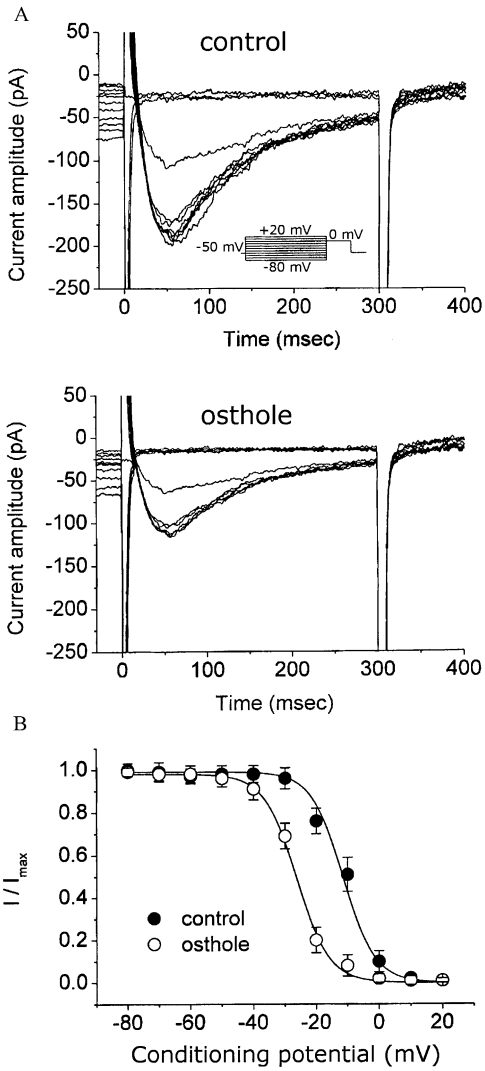

Fig. 4. Steady state inactivation curve of $I_{Ca,L}$ in the absence and presence of osthole. With the aid of a double-pulse protocol, the steady state inactivation parameters of $I_{Ca,L}$ were obtained in the absence and presence of osthole (3 μM). The conditioning voltage pulses with a duration of 1 s to various membrane potentials between −80 and +20 mV were applied from a holding potential of −50 mV. Following each conditioning pulse, a test pulse to 0 mV with a duration of 300 ms was applied to evoke $I_{Ca,L}$. (A) Superimposed current traces in the absence (upper part) and presence (lower part) of osthole (3 μM). Inset shown in (A) indicates the voltage protocol. (B) Steady state inactivation curves of $I_{Ca,L}$ obtained in the absence (filled circles) and presence (open circles) of osthole (3 μM). The normalized amplitude of $I_{Ca,L}$ (I/I_{max}) was constructed against the conditioning potential and the curves were fitted by the Boltzmann equation (see text for details).

(3 μM). A two-step voltage pulse protocol was applied [18]. A 1 s conditioning pulse to various membrane potentials preceded the test pulse (300 ms in duration) to 0 mV from a holding potential of −50 mV. The interval between two sets of voltage pulses was 60 s to prevent incomplete recovery of $I_{Ca,L}$. The relationships between the membrane potentials and the normalized amplitudes of $I_{Ca,L}$ with or without addition of osthole (3 μM) were plotted and fitted to a Boltzmann function using non-linear regression analysis [16,18]: $I = I_{max}/\{1 + \exp[(V - a)/b]\}$, where I_{max} is the maximal activated $I_{Ca,L}$, V the membrane potential in mV, a the membrane potential for half-maximal inactivation and b is the slope factor of inactivation curve. In control, $a = -11.4 \pm 0.9$ mV, $b = 5.1 \pm 0.4$ mV ($N = 7$), whereas in the presence of osthole (3 μM), $a = -26.2 \pm 1.5$ mV, $b = 5.2 \pm 0.4$ mV ($N = 6$). It appeared, therefore, that the presence of osthole not only suppressed the maximal conductance of $I_{Ca,L}$, but also shifted the inactivation curve to a hyperpolarized potential by approximately −15 mV. However, we found no significant change in the slope of the curve during cell exposure to osthole. These results clearly indicate that osthole can suppress the amplitude of $I_{Ca,L}$ in a voltage-dependent manner in NG108-15 cells.

3.4. Effect of osthole on the recovery of $I_{Ca,L}$ from inactivation

The effect of osthole on the recovery of $I_{Ca,L}$ from inactivation was studied with a double-pulse protocol. The recovery of $I_{Ca,L}$ from inactivation at a holding potential of −50 mV was examined at different times with a test step (0 mV for 300 ms). As shown in Fig. 5, in the control, the amplitude of peak inward current almost completely recovered from inactivation when the recovery time was 5 s. The time course of recovery from inactivation in the control was fitted to a single-exponential function with a time constant of 1.28 ± 0.11 s ($N = 6$). However, in the presence of osthole (3 μM), the recovery from inactivation was significantly prolonged with a time constant of 3.31 ± 0.23 s ($N = 6$). After a 5 s interval, the amplitude of peak inward current was found to completely recover from inactivation in the control; however, in the presence of osthole, a substantial block of peak inward current was still observed (Fig. 5). Therefore, the presence of osthole caused a significant prolongation of the recovery from inactivation of $I_{Ca,L}$ in NG108-15 cells. In other words, there is a slow recovery from inactivation in the presence of osthole.

3.5. Lack of effect of osthole on voltage-dependent K^+ outward current (I_K) in NG108-15 cells

We also examined whether osthole affects the amplitude of I_K in these cells. In these experiments, cells were bathed in Ca^{2+}-free Tyrode's solution containing 1 μM tetrodotoxin and 0.5 μM $CdCl_2$. When the cell was held at −50 mV and various potentials ranging from −40 to +60 mV in 10 mV increments were applied at a rate of 0.05 Hz, no significant difference in current amplitudes at each voltage step between the absence and presence of osthole (100 μM) could be demonstrated (Fig. 6). Similar results were obtained in seven different cells. However, TEA (10 mM), quinidine (10 μM) and dendrotoxin (1 μM) produced an effective inhibition in the amplitude of I_K. TEA, quinidine and dendrotoxin are blockers of I_K in a variety of cells [19,20]. TEA has also been shown to selectively block Ca^{2+}-activated K^+ channels in arterial smooth muscle cells at concentration less than 1 mM [21]. Thus, it is clear that unlike $I_{Ca,L}$, voltage-dependent I_K was unaffected by osthole in NG108-15 cells.

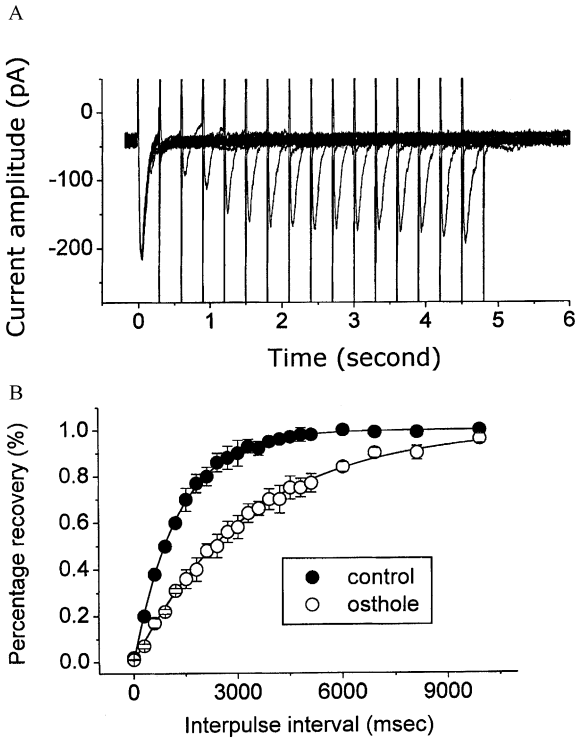

Fig. 5. Effect of osthole on the recovery of $I_{Ca,L}$ from inactivation in NG108-15 cells. The cells were depolarized from −50 to +10 mV with a duration of 300 ms and various interpulse durations were applied. An example of current traces obtained by a two-pulse protocol in the control (i.e. the absence of osthole) is illustrated in (A). (B) Effect of osthole on the time course of recovery from the inactivation of $I_{Ca,L}$ after the cells were depolarized from −50 to +10 mV. Filled symbols are in control and open symbols were obtained 2 min after addition of osthole (3 μM). Each smooth line was fitted by a single-exponential function.

3.6. Effect of osthole on spontaneous spiking discharge of NG108-15 cells

In an additional series of experiments, we examined the effect of osthole on changes in membrane potential of NG108-15 cells. NG105-18 cells, bathed in normal Tyrode's solution containing 1.8 mM $CaCl_2$, had a resting membrane potential of -53 ± 6 mV ($N = 24$) under a

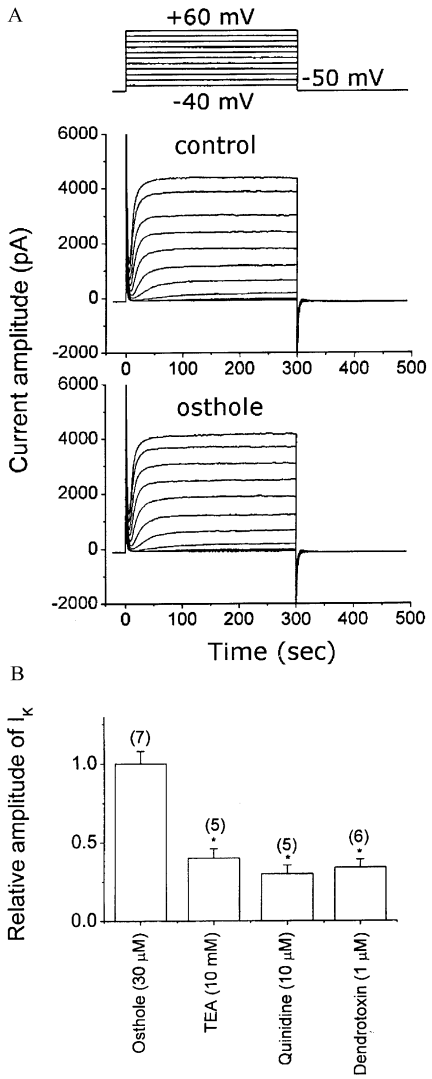

Fig. 6. Lack of effect of osthole on I_K in NG108-15 cells. Cells, bathed in Ca^{2+}-free Tyrode's solution containing tetrodotoxin (1 μM) and $CdCl_2$ (0.5 mM), were held at −50 mV and the voltage pulses from −40 to +60 mV in 10 mV increments were applied at a rate of 0.05 Hz. In (A), superimposed current traces shown in upper part are control, and those in lower part were recorded 2 min after addition of osthole (100 μM). Voltage protocol is shown in upper part. (B) Comparison between the effect of osthole (100 μM) and those of tetraethylammonium chloride (10 mM; TEA), quinidine (10 μM), and dendrotoxin (1 μM) on the amplitude of I_K. Each cell was depolarized from −50 to +50 mV. The amplitude of I_K measured at the end of the voltage pulses in the control was considered to be 1.0 and the relative amplitude of I_K after addition of each agent was plotted. *Significantly different from control ($P < 0.05$).

current-clamp configuration. The typical effects of osthole on membrane potentials in these cells are illustrated in Fig. 7. Under our experimental conditions, about 60% of NG105-18 cells was noted to exhibit a repetitive firing of action potentials that was Ca^{2+}-sensitive and inhibited by nimodipine, yet not by tetrodotoxin. When osthole (10 μM) was applied to the bath, spontaneous spiking discharge seen in these cells was significantly decreased from 0.52 ± 0.05 to 0.09 ± 0.02 Hz ($N = 7$). However, no significant change in resting membrane potential was observed (-53 ± 8 vs. -50 ± 7 mV, $N = 7$, $P > 0.05$). When osthole was washed out, spontaneous action potential was returned. In contrast, ω-conotoxin GVIA (3 μM) had no significant effect on the firing of action potentials (Fig. 7B). However, the application of osthole (10 μM) in the continued presence of ω-conotoxin GVIA also decreased the firing frequency (data not shown). Thus, it is clear that, similar to nimodipine, osthole can regulate the firing of action potentials in NG108-15 cells.

4. Discussion

The major findings of this study are as follows. First, in NG108-15 neuronal cells, osthole inhibits $I_{Ca,L}$ in a concentration- and voltage-dependent manner. Second, it is unlikely that the effect of osthole on $I_{Ca,L}$ is mediated by an inhibition of the activities of phosphodiesterases. Third, osthole can produce a negative shift in the steady state inactivation curve of $I_{Ca,L}$. Fourth, osthole can modify the firing of action potentials in these cells. These results suggest that osthole can interact directly with L-type Ca^{2+} channels in NG108-15 cells and that inhibition of the these channels can be one of the ionic mechanisms underlying osthole-induced change in functional activity of neurons or neuroendocrine cells.

The present study provides direct evidence that osthole inhibits the amplitude of $I_{Ca,L}$ in NG108-15 neuronal cells in a concentration-dependent fashion. The IC_{50} value of osthole required for the inhibition of $I_{Ca,L}$ was 4 μM. In rat thoracic aorta and guinea pig trachea, it has been reported that osthole-inhibited KCl-induced contraction with a concentration range of 20–100 μM [4,5]. This value seems to be greater than the present data obtained from NG108-15 neuronal cells. However, a recent report by Chiou *et al.* showed that osthole-inhibited phenylephrine-induced contraction of rabbit corpus cavernosum with an IC_{50} value of about 2 μM [8]. The IC_{50} value needed to exert antiproliferative effect on rat vascular smooth muscle cells was reported to be approximately 10 μM [22]. In addition, we could find no evidence that osthole had any effect on voltage-dependent I_K in NG108-15 cells. Therefore, L-type Ca^{2+} channels present in neurons or neuroendocrine cells are likely to be the targets of osthole, since the effect of osthole observed in our experiments appeared to occur at a concentration achievable in rat plasma [23].

In this study, we found that the presence of osthole caused a prolongation of the recovery from inactivation of $I_{Ca,L}$ in NG108-15 cells. These results suggest that the recovery from inactivation was slower in the presence of osthole. In addition, the present results demonstrated that osthole not only reduced the maximal conductance of $I_{Ca,L}$, but it also produced a distinct shift in the steady state inactivation curve. Such a shift can be explained by: (a) the binding of osthole to the inactivated state and (b) state-independent binding of osthole that would result in an

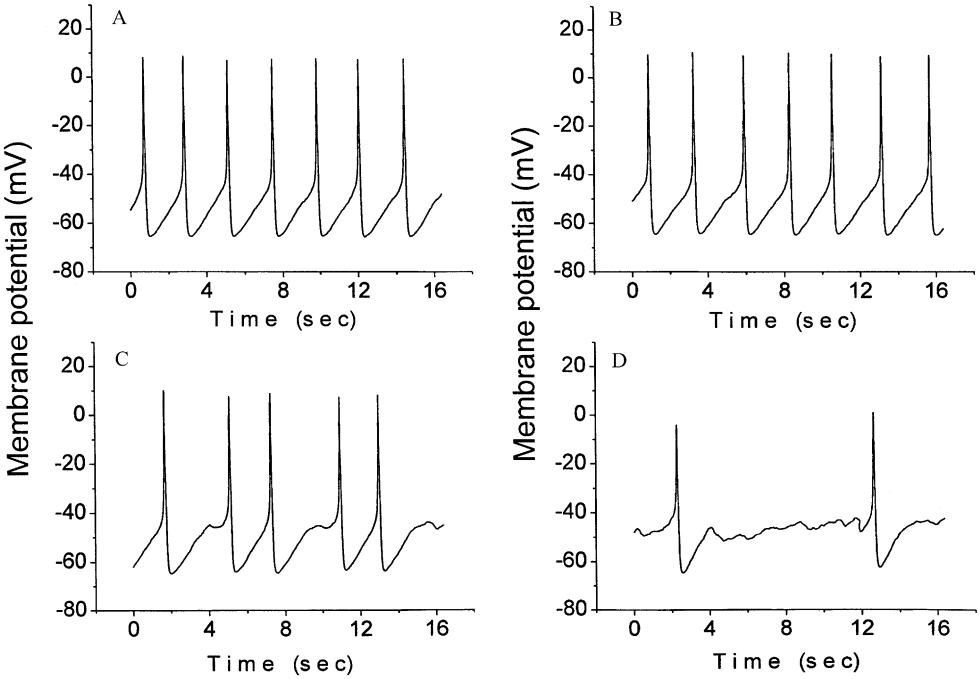

Fig. 7. Effect of osthole on spontaneous action potentials of NG108-15 cells. Cells were bathed in normal Tyrode's solution containing 1.8 mM $CaCl_2$. The patch pipettes were filled with K^+-containing solution. The experiments were conducted under current-clamp conditions. (A) control; (B) ω-conotoxin GVIA (3 μM); (C) osthole (3 μM); (D) osthole (10 μM). Notably, osthole decreases the firing frequency of spontaneous action potentials in these cells.

accelerated transition of the channels to the inactivated state. However, the exact location of the binding site on L-type Ca^{2+} channels for osthole remains to be determined. In addition, the results showing osthole-induced a shift in the inactivation curve suggest that the inhibitory effect of osthole on $I_{Ca,L}$ is voltage-dependent and that the magnitude of current inhibition caused by osthole can be altered by changes in membrane potential. Indeed, these observations can be interpreted to be consistent with a previous finding demonstrating that osthole alone had no effect on resting tension and Ca^{2+} influx in rat thoracic aorta, but it preferentially inhibited the contraction during the K^+-induced depolarization [4]. Therefore, the sensitivity to osthole in neurons would be dependent on the preexisting level of resting membrane potential, the firing rate of action potentials, or the concentration of osthole used [24].

It has previously been reported that the action of osthole appeared to be associated with an increase in the level of intracellular cyclic AMP and GMP, because it might inhibit the activities of cyclic nucleotide phosphodiesterases [1,5,7,22]. However, this study showed that sp-cAMPS, a cell permeable analogue of cyclic AMP, had no effect on the amplitude of $I_{Ca,L}$ in NG108-15 cells, whereas 8-bromo-cGMP suppressed $I_{Ca,L}$ only by 15%. Therefore, it is reasonable to assume that the inhibitory effects of osthole on Ca^{2+} currents observed in this study will not involve changes in the level of cyclic AMP or GMP.

Osthole can modulate the membrane potential of NG108-15 cells by a direct inhibition of $I_{Ca,L}$. Despite a number of studies showed that osthole could suppress the activities of cyclic nucleotide phosphodiesterases [1,5,7, 22], the osthole-mediated regulation of spontaneous action potentials observed in NG108-15 cells also did not appear to be a consequence of its effect on change in the level of intracellular cyclic AMP or GMP. In fact, the inhibitory effect on spontaneous action potentials by osthole was primarily due to the block of dihydropyridine-sensitive L-type Ca^{2+} channels, because ω-conotoxin GVIA had no effect on the firing of action potentials in these cells. Therefore, the inhibition of $I_{Ca,L}$ and a concomitant reduction in the firing of actions potentials by osthole might confuse the interpretation of results drawn from studies of signal transduction which use osthole as an inhibitor of cyclic nucleotide phosphodiesterases [5,7].

It has been reported that NG108-15 neuronal cells exhibited at least two types of Ca^{2+} channel contributing to high-threshold Ca^{2+} current: an ω-conotoxin GVIA-resistant, dihydropyridine-sensitive type, an ω-conotoxin GVIA-sensitive, dihydropyridine-resistant type [9,10]. The major part of osthole-inhibited Ca^{2+} current in undifferentiated NG108-15 cells seen in this study appeared to be due to the block of dihydropyridine-sensitive L-type Ca^{2+} channels, rather than neuronal N-type channels. Indeed, ω-conotoxin GVIA. a potent blocker of N-type channels and a weak blocker of L-type channels [17], did not suppress Ca^{2+} current that was sensitive to the inhibition by osthole. Previous studies have shown that extracellular Ca^{2+} influx occurs mainly through N-type channels and these channels present in neurons play an

important role in neurotransmitter release [25]. However, recent studies indeed suggested that the activity of L-type channels present in neurons might involve the modulation of glutamate-induced burst firing or anoxia-mediated Ca^{2+} influx [26,27]. Thus, osthole-mediated inhibition of $I_{Ca,L}$ would play a role in the regulation of neuronal activity.

In summary, results from the present study indicate that the major part of osthole-mediated inhibition of Ca^{2+} current in NG108-15 cells was primarily due to the block of dihydropyridine-sensitive L-type Ca^{2+} channels. Accordingly, we found that osthole abolished Ca^{2+}-sensitive action potential via the inhibition of L-type Ca^{2+} channel. The effects of osthole may not solely be due to its inhibition of the activities of phosphodiesterases. Osthole also appears to be another pharmacological tool used to isolate L-type components of I_{Ca} in excitable cells. If the mechanism of inhibitory actions of osthole on $I_{Ca,L}$ found in NG108-15 neuronal cells exists in intact brain neurons, this compound may reduce Ca^{2+} influx resulting from the inhibition of L-type Ca^{2+} channels.

Acknowledgments

We would like to thank Pei-Hsuan Lin and Yen-Hua Hung for their technical assistance. This work was supported by grants from the National Science Council (NSC-89-2320-B075B-016), Kaohsiung Veterans General Hospital (VGHKS90-06, and VGHKS90-73), and VTY Joint Research Program, Tsou's Foundation (VTY-89-P3-23), Taiwan, ROC.

References

[1] Hoult JR, Paya M. Pharmacological and biochemical actions of simple coumarins: natural products with therapeutic potential. Gen Pharmacol 1996;27:713–22.

[2] Liu SX, Chiou GC. Effects of Chinese herbal products on mammalian retinal functions. J Ocul Pharmacol Ther 1996;12:377–86.

[3] Ko FN, Wu TS, Liou MJ, Huang TF, Teng CM. Inhibition of platelet thromboxane formation and phosphoinositides breakdown by osthole from Angelica pubescens. Thromb Haemost 1989;62:996–9.

[4] Ko FN, Wu TS, Liou MJ, Huang TF, Teng CM. Vasorelaxation of rat thoracic aorta caused by osthole isolated from Angelica pubescens. Eur J Pharmacol 1992;219:29–34.

[5] Teng CM, Lin CH, Ko FN, Wu TS, Huang TF. The relaxant action of osthole isolated from Angelica pubescens in guinea pig trachea. Naunyn-Schmied Arch Pharmacol 1994;349:202–8.

[6] Li L, Zhuang FE, Yang L, Zhang CL, Zhao GS, Zhao DK. Effects of osthole on isolated guinea pig heart atria. Zhongguo Yao Li Xue Bao 1995;16:251–4.

[7] Chen J, Chiou WF, Chen CC, Chen CF. Effect of the plant-extract osthole on the relaxation of rabbit corpus cavernosum tissue in vitro. J Urol 2000;163:1975–80.

[8] Chiou WF, Huang YL, Chen CF, Chen CC. Vasorelaxant effect of coumarins from *Cnidium monnieri* on rabbit corpus cavernosum. Planta Med 2001;67:1–3.

[9] Kasai H, Neher E. Dihydropyridine-sensitive and ω-conotoxin-sensitive calcium channels in a mammalian neuroblastoma–glioma cell line. J Physiol 1992;448:161–88.

[10] Seabrook GR, McAllister G, Knowles MR, Myers J, Sinclair HA, Patel S, Freedman SB, Kemp JA. Depression of high-threshold calcium currents by activation of human $D_{2(short)}$ dopamine receptors expressed in differentiated NG108-15 cells. Br J Pharmacol 1994;111:1061–6.

[11] Brown NA, Seabrook GR. Phosphorylation and voltage-dependent inhibition of neuronal calcium currents by activation human $D_{2(short)}$ dopamine receptors. Br J Pharmacol 1995;115:459–66.

[12] Lukyanetz EA, Piper TP, Sihra TS. Calcineurin involvement in the regulation of high-threshold Ca^{2+} channels in NG108-15 (rodent neuroblastoma × glioma hybrid) cells. J Physiol 1998;510:371–85.

[13] Hashii M, Minabe Y, Higashida H. cADP-ribose potentiates cytosolic Ca^{2+} elevation and Ca^{2+} entry via L-type voltage-activated Ca^{2+} channels in NG108-15 neuronal cells. Biochem J 2000;345:207–15.

[14] Hamill OP, Marty A, Neher E, Sackmann B, Sigworth FJ. Improved patch-clamp techniques for high resolution current recording from cells and cell-free membrane patches. Pflügers Arch 1981;391:85–100.

[15] Wu SN, Hwang TL, Jan CR, Tseng CJ. Ionic mechanisms of tetrandrine in cultured rat aortic smooth muscle cells. Eur J Pharmacol 1997;327:233–8.

[16] Wu SN, Shen AY, Hwang TL. Analysis of mechanical restitution and post-rest potentiation in isolated rat atrium. Chin J Physiol 1996;39:23–9.

[17] Williams ME, Feldmann DH, McCue AF, Brenner R, Velicelebi G, Ellis SB, Harpold MM. Structure and functional expression of α_1, α_2 and β subunits of a novel human neuronal calcium channel subtype. Neuron 1992;8:71–84.

[18] Lo YC, Wu SN, Wu JR, Chen IJ. Effect of capsaicin on membrane currents in cultured vascular smooth muscle cells of rat aorta. Eur J Pharmacol 1995;292:321–8.

[19] Kraliz D, Bhattacharya A, Singh S. Blockade of the delayed rectifier potassium current in *Drosophila* by quinidine and related compounds. J Neurogenet 1998;12:25–39.

[20] Wang FC, Bell N, Reid P, Smith LA, McIntosh P, Robertson B, Dolly JO. Identification of residues in dendrotoxin K responsible for its discrimination between neuronal K^+ channels containing Kv1.1 and 1.2 alpha subunits. Eur J Biochem 1999;263:222–9.

[21] Langton PD, Nelson MT, Huang Y, Standen NB. Block of calcium-activated potassium channels in mammalian arterial myocytes. Am J Physiol 1991;260:H927–934.

[22] Guh JH, Yu SM, Ko FN, Wu TS, Teng CM. Antiproliferative effect in rat vascular smooth muscle cells by osthole, isolated from Angelica pubescens. Eur J Pharmacol 1996;298:191–7.

[23] Tsai TH, Tsai TR, Chen CC, Chen CF. Pharmacokinetics of osthole in rat plasma using high-performance liquid chromatography. J Pharm Biomed Anal 1996;14:749–53.

[24] Spedding M, Kenny B, Chatelain P. New drug binding sites in Ca^{2+} channels. Trends Pharmacol Sci 1995;16:139–42.

[25] Hirning LD, Fox AP, McCleskey EW, Olivera BM, Thayer SA, Miller RJ, Tsien RW. Dominant role of N-type Ca^{2+} channels in evoked release of norepinephrine from sympathetic neurons. Science 1988;239:57–61.

[26] Cooper DC, White FJ. L-type calcium channels modulate glutamate-driven bursting activity in the nucleus accumbens *in vivo*. Brain Res 2000;880:212–8.

[27] Brown AM, Westenbroek RE, Catterall WA, Ransom BR. Axonal L-type Ca^{2+} channels and anoxic injury in rat CNS white matter. J Neurophysiol 2001;85:900–11.